

Novel Polar Single Amino Acid Chelates for Technetium-99m Tricarbonyl-Based Radiopharmaceuticals with Enhanced Renal Clearance: Application to Octreotide

Kevin P. Maresca, John C. Marquis, Shawn M. Hillier, Genliang Lu, Frank J. Femia, Craig N. Zimmerman, William C. Eckelman, John L. Joyal, and John W. Babich*

Molecular Insight Pharmaceuticals, Inc., 160 Second Street, Cambridge, Massachusetts 02142. Received November 23, 2009; Revised Manuscript Received March 10, 2010

Single amino acid chelate (SAAC) systems for the incorporation of the $M(\text{CO})_3$ moiety ($M = \text{Tc/Re}$) have been successfully incorporated into novel synthetic strategies for radiopharmaceuticals and evaluated in a variety of biological applications. However, the lipophilicity of the first generation $\text{Tc}(\text{CO})_3$ -dipyridyl complexes has resulted in substantial hepatobiliary uptake when either examined as lysine derivatives or integrated into biologically active small molecules and peptides. Here we designed, synthesized, and evaluated novel SAAC systems that have been chemically modified to promote overall $\text{Tc}(\text{CO})_3\text{L}_3$ complex hydrophilicity with the intent of enhancing renal clearance. A series of lysine derived SAAC systems containing functionalized polar imidazole rings and/or carboxylic acids were synthesized via reductive alkylation of the ϵ amino group of lysine. The SAAC systems were radiolabeled with $^{99\text{m}}\text{Tc}$, purified, and evaluated for radiochemical stability, lipophilicity, and tissue distribution in rats. The $\log P$ values of the $^{99\text{m}}\text{Tc}$ complexes were determined experimentally and ranged from -0.91 to -2.33 . The resulting complexes were stable ($>90\%$) for at least 24 h. Tissue distribution in normal rats of the lead $^{99\text{m}}\text{Tc}$ complexes demonstrated decreased liver ($<1\% \text{ID/g}$) and gastrointestinal clearance ($<1.5\% \text{ID/g}$) and increased kidney clearance ($>15\% \text{ID/g}$) at 2 h after injection compared to the dipyridyl lysine complex (DpK). One of the new SAAC ligands, [$^{99\text{m}}\text{Tc}$]bis-carboxymethylimidazole lysine, was conjugated to the N-terminus of Tyr-3 octreotide and evaluated for localization in nude mice bearing AR42J xenografts to examine tissue distribution, tumor uptake and retention, clearance, and route of excretion for comparison to ^{111}In -DOTA-Tyr-3-octreotide and $^{99\text{m}}\text{Tc}$ -DpK-Tyr-3-octreotide. $^{99\text{m}}\text{Tc}$ -bis-(carboxymethylimidazole)-lysine-Tyr-3-octreotide exhibited significantly less liver uptake and gastrointestinal clearance compared to $^{99\text{m}}\text{Tc}$ -DpK-Tyr-3-octreotide while maintaining tumor uptake in the same mouse model. These novel chelators demonstrate that lipophilicity can be controlled and organ distribution significantly altered, opening up broad application of these novel SAAC systems for radiopharmaceutical design.

INTRODUCTION

The potential to employ the radionuclide technetium-99m with its optimal decay characteristics into targeting molecules has been the foremost consideration in developing diagnostic radiopharmaceuticals (1–3). $^{99\text{m}}\text{Tc}$ -labeled radiopharmaceuticals are preferred over other isotopes because of the ideal nuclear properties of the isotope, as well as its widespread availability from commercial generator columns. $^{99\text{m}}\text{Tc}$ emits a 140 keV γ -ray with 89% abundance, which is ideal for imaging with commercial γ cameras. Furthermore, the combination of the medically useful radionuclides, $^{99\text{m}}\text{Tc}$ and rhenium-186/188 ($^{186/188}\text{Re}$), which have remarkably similar coordination chemistries in terms of the $\{M(\text{CO})_3\text{L}_3\}^+$ core thereby yielding isostructural coordination complexes with favorable physical decay characteristics, is attractive for molecular imaging and radiotherapy, respectively (4, 5).

We previously described a technology known as the single amino acid chelate (SAAC) (6), a radiolabeling platform that has broad utility in radiochemical, fluorescent and dual modality (radio/fluorescent) molecular imaging. SAAC ligands are novel bifunctional chelates constructed from derivatized amino acids modified to provide three donor groups (L_3) for chelation to the $\{M(\text{CO})_3\}^{1+}$ core ($M = \text{Tc}$ or Re). SAAC derivatives demonstrate facile labeling with $^{99\text{m}}\text{Tc}$ and robust complex stability toward cysteine and histidine challenges, which present major *in vivo* competition for these ligands (7). SAAC avoids

the many problems associated with using sulfhydryl containing radioligands and chelating agents that do not fully occupy the coordination sites of Tc and Re or form unstable complexes. In addition, SAAC may be incorporated into bioactive peptides via standard solid phase peptide synthesis and subsequently labeled with $^{99\text{m}}\text{Tc}$ and $^{186/188}\text{Re}$ (8, 9).

During the past decade, the field of technetium coordination chemistry has seen both a rising interest in the Tc(I) core (10–15) and diminishing expectations for its utility, as the core and the subsequent chelators have demonstrated significant deficiencies (16, 17). These shortcomings, most notably the hydrophobicity of the metal complexes, are inherent characteristics of the core itself, which are exaggerated by the very nature of the chelators that form the robust complexes. Unfortunately, the lipophilicity of the chelators typically contributes to a poor pharmacokinetic profile of the radiotracer characterized by hepatic accumulation or hepatobiliary clearance. The ability to capitalize on the synthetic flexibility of incorporation, and the stability and inertness of the Tc(I) core, while decreasing the lipophilicity is key to the future success of the technology.

One potential solution to overcome the high hepatobiliary clearance of the complexes is to decrease the lipophilicity surrounding the metal center. Two possible ways to address this issue include (i) derivatizing the metal coordinating ligands with polar, nonlipophilic substituents to counterbalance the lipophilic metal-chelate core or (ii) decreasing the overall size of the ligands used to coordinate the metal core (18, 19). The former may be accomplished by modifying imidazole SAAC systems

* Corresponding author.

with polar, water-solubilizing functional groups such as ethers, alcohols, and carboxylic acids, which should alter the pharmacokinetic properties of the SAAC systems, and the biologically relevant molecules to which they are conjugated. In addition, these substitutions will result in metal complexes with neutral, cationic, or anionic charges of the metal complex, which may impact the pharmacokinetic profile. Alternatively, replacing one or more of the ligand donor heteroaromatic rings with a smaller, less hydrophobic donor, i.e., acetic acid, will reduce the size and lipophilicity of the complexes. For example, the nitrilotriacetic acid chelate (NTA) reported by Lipowska et al. (20) favored tubular transport rather than hepatobiliary excretion.

In an attempt to address the undesirable liver and gastrointestinal uptake and clearance characteristic of many of the SAAC systems previously designed and evaluated in our laboratory, we have investigated functionalized polar lysine imidazole derivatives with the potential to enhance renal clearance. These novel imidazole SAAC systems can be synthesized with a variety of hydrophilic R-groups via alkylation of imidazole-2-carboxaldehyde with available alkyl halides that contain the desired polar functionality (21). In previous work, we functionalized imidazole ligands with ether-containing moieties to investigate cardiac imaging (22) resulting in complexes with very low liver uptake and retention. These same principles, expanded to include various alcohols, ethers, and acids, were applied to the SAAC systems to shift the current pharmacokinetic profile from hepatobiliary uptake to higher renal clearance.

Here we describe the synthesis and evaluation of a series of lysine derived SAAC systems with a variety of metal donor ligand groups to form (2-amino-6-(bis((1-X-1*H*-imidazol-2-yl)methyl)amino)hexanoic acid) where X = methyl (1), 2,2-dimethoxyethyl (2), 2-ethoxyethyl (3), carboxymethyl (4), 2-hydroxyethyl (5), 3-(diethoxyphosphoryl)propyl (6), as well as (*S*)-2-amino-6-((carboxymethyl)(thiazol-2-ylmethyl)amino)hexanoic acid (7), (*S*)-2-amino-6-((carboxymethyl)(1-methyl-1*H*-imidazol-2-yl)methyl)amino)hexanoic acid (8), 2,2'-(5-amino-5-carboxypentylazanediyl)diacetic acid (9) and compared them to 2-amino-6-(bis(pyridin-2-ylmethyl)amino)hexanoic acid (DpK) and 2-amino-6-((carboxymethyl)(pyridin-2-ylmethyl)amino)hexanoic acid (PAMAK). Tissue distribution data obtained with these complexes in normal rats demonstrated greater kidney clearance and significantly less liver and gastrointestinal uptake than first generation SAAC ligands. Two SAAC ligands were subsequently incorporated using solid phase peptide synthesis into Tyr-3-octreotide yielding, ^{99m}Tc-4-Tyr-3-octreotide and ^{99m}Tc-DpK-Tyr-3-octreotide. These peptides were evaluated for localization in nude mice bearing AR42J xenografts to examine tissue distribution, tumor uptake and retention, clearance, and route of excretion for comparison to ¹¹¹In-DOTA-Tyr-3-octreotide, a well established radioimaging agent with excellent pharmacokinetic properties that targets the type 2 somatostatin receptor in neuroendocrine tumors (23–25).

EXPERIMENTAL SECTION

General Methods. All reactions were carried out in dry glassware under an atmosphere of argon unless otherwise noted. Reactions were purified by column chromatography under medium pressure using a Biotage SP4 or by preparative high pressure liquid chromatography using a Varian Prostar 210 preparative high pressure liquid chromatography (HPLC) system equipped with a semipreparative Vydac C18 reverse-phase column (250 mm × 10 mm × 5 μm) connected to a Varian Prostar model 320 UV-visible detector and monitored at a wavelength of 254 nm. The final technetium SAAC complexes were purified and analyzed using a binary solvent gradient of 5–95% buffer B over 21 min (buffer A = triethylammonium phosphate (TEAP), pH 3, buffer B = methanol). The final ^{99m}Tc-

SAAC-peptide conjugates were purified and analyzed on Vydac C18 reverse-phase column (250 mm × 4.6 mm × 5 μm) employing a gradient method of 5–50% buffer B over 30 min (buffer A = water + 0.1% TFA, buffer B = acetonitrile + 0.1% TFA). ¹H NMR spectra were obtained on a Bruker 400 MHz instrument. Spectra are reported as ppm and are referenced to the solvent resonances in chloroform-*d* (CDCl₃), dimethyl sulfoxide-*d*₆ (DMSO-*d*₆), or methanol-*d*₄ (MeOD). Combustion analyses were performed by Prevalere Life Sciences, Inc. ^{99m}Tc was used as a solution of Na^{99m}TcO₄ in saline, as a commercial ⁹⁹Mo/^{99m}Tc generator eluant (Cardinal Health). The ^{99m}Tc-containing solutions were always kept behind sufficient lead shielding. The [^{99m}Tc(CO)₃(H₂O)₃]⁺ was prepared from commercially available Isolink kits (Covidien). The ¹¹¹In was used as an ¹¹¹InCl₃ solution commercially available from MDS Nordion. All solvents and reagents were purchased from Sigma Aldrich (St. Louis, MO), Bachem (Switzerland), Akaal (Long Beach, CA), or Anaspec (San Jose, CA). The following abbreviations are used: Fmoc = fluorenylmethoxycarbonyl, DMAP = *N,N*-dimethylaminopyridine, DMF = *N,N*-dimethylformamide, DMSO = dimethyl sulfoxide, DCM = dichloromethane, DCE = 1,2-dichloroethane, NaOH = sodium hydroxide, (*S*)-2-(((9*H*-fluoren-9-yl)methoxy)carbonylamino)-6-aminohexanoic acid hydrochloride salt = L-Fmoc-lysine-OH hydrochloride salt, ID/g = injected dose per gram, NTA = nitrilotriacetic acid, PBS = phosphate buffered saline, RCP = radiochemical purity, RCY = radiochemical yield.

Syntheses. General Procedure for the Alkylations. To a solution of the imidazole-2-carboxaldehyde dissolved in DMF (1 mL) was added 1 mol equiv of the alkyl bromide, excess potassium carbonate, and a catalytic amount of potassium iodide. The mixture was heated at 110 °C for 18 h followed by evaporation to dryness and purified utilizing a Biotage SP4 with a gradient method of 5–50% methanol in DCM.

General Procedure for the Reductive Aminations. To a solution of L-Fmoc-lysine-OH hydrochloride salt (90 mg, 0.19 mmol) dissolved in DCE (2 mL) was added 2.1 equiv of the aldehyde. The mixture was heated at 50 °C for 1 h whereupon sodium triacetoxyborohydride (36 mg, 0.19 mmol) was added. The mixture was stirred at room temperature for 12 h and was subsequently evaporated to dryness and purified utilizing a Biotage SP4 with a gradient method of 5–50% methanol in DCM. The purified compound (24 mg, 0.034 mmol) was deprotected by treatment with piperidine/DMF 1:1 (1 mL), and the mixture was stirred at room temperature for 2 h. Following evaporation to residue, aqueous extraction and washing with excess DCM afforded the desired compounds as an off-white solid.

(*S*)-2-Amino-6-(bis((1-methyl-1*H*-imidazol-2-yl)methyl)amino)hexanoic Acid (1). A solution of Fmoc-Lys-OH·HCl (1.8 g, 4.5 mmol) and 1-methyl-1*H*-imidazole-2-carbaldehyde (1.1 g, 10 mmol) in DCE (50 mL) was stirred at 75 °C for 30 min under nitrogen. The reaction mixture was cooled to 0 °C and treated with sodium triacetoxyborohydride (3.2 g, 15 mmol). The reaction mixture was stirred at room temperature overnight and was decomposed with water. The reaction mixture was extracted with DCM. The organic layer was dried and concentrated under reduced pressure. The residue was purified by flash chromatography over silica gel to afford (*S*)-2-(((9*H*-fluoren-9-yl)methoxy)carbonylamino)-6-(bis((1-methyl-1*H*-imidazol-2-yl)methyl)amino)hexanoic acid (2.3 g, 92%). MS (ESI), 557 (M + H)⁺. To a solution of (*S*)-2-(((9*H*-fluoren-9-yl)methoxy)carbonylamino)-6-(bis((1-methyl-1*H*-imidazol-2-yl)methyl)amino)hexanoic acid (556 mg, 1.00 mmol) in DMF (4.0 mL) was added piperidine (0.80 mL). The mixture was stirred at room temperature for 2 h. Solvent was evaporated under reduce pressure to afford a residue, which was purified by Amberchrom column chromatography to afford (*S*)-2-

amino-6-(bis((1-methyl-1*H*-imidazol-2-yl)methyl)amino)hexanoic acid (320 mg, 0.958 mmol, 96% yield). ¹H NMR (400 MHz, DMSO-*d*₆) δ 7.94 (s, 1 H), 7.04 (d, *J* = 3, 1.2 Hz, 2H), 6.74 (d, *J* = 1.2 Hz, 2 H), 3.54 (s, 4 H), 3.98 (brs, 1 H), 2.88 (s, 3 H), 2.72 (s, 3 H), 2.35 (t, *J* = 6.8 Hz, 2 H), 1.60–1.54 (m, 1 H), 1.43–1.29 (m, 3 H), 1.16–1.11 (m, 2 H). MS (ESI): 335 (M + H)⁺.

*1-(2,2-Dimethoxyethyl)-1*H*-imidazole-2-carbaldehyde (2A)*. To a solution of the imidazole-2-carboxaldehyde (410 mg, 4.3 mmol) dissolved in DMF (1 mL) was added 1.1 equiv of 2-bromo-1,1-dimethoxyethane (800 mg, 4.7 mmol), potassium carbonate, and a catalytic amount of potassium iodide. The mixture was heated at 110 °C for 18 h followed by evaporation to dryness and purified utilizing a Biotage SP4 with a gradient method of 5–50% methanol in DCM to yield the desired compound (250 mg, 1.4 mmol, 32% yield). ¹H NMR (400 MHz, DMSO-*d*₆) δ 9.9 (s, H), 7.85 (s, H), 7.55 (s, H), 5.82 (m, H), 4.75 (d, 2H), 3.45 (s, 6H).

*(S)-2-Amino-6-(bis((1-(2,2-dimethoxyethyl)-1*H*-imidazol-2-yl)methyl)amino)hexanoic Acid (2)*. Following the same procedure as utilized in the preparation of **1** yielded the desired compound (93 mg, 0.132 mmol, 54% yield). ¹H NMR (400 MHz, DMSO-*d*₆) δ 7.90 (d, 2H), 7.72 (d, 2H), 7.41 (m, 2H), 7.30 (m, 2H), 7.05 (s, H), 6.75 (s, H), 4.45 (m, 3H), 4.2 (m, 4H), 3.95 (d, 2H), 3.80 (m, H), 3.55 (s, 2H), 3.2 (s, 6H), 2.3 (m, 2H), 1.60 (m, H), 1.35 (m, H), 1.15 (m, 2H). ESMS *m/z*: 705 (M + H)⁺.

The purified compound was deprotected by treatment with piperidine/DMF 1:1 (1 mL), and the mixture was stirred at room temperature for 18 h. Following evaporation to residue, aqueous extraction from DCM afforded the desired product (44 mg, 0.093 mmol, 76% yield) as an off-white solid. ¹H NMR (400 MHz, DMSO-*d*₆) δ 7.98 (s, H), 7.05 (s, H), 6.85 (s, H), 4.45 (s, 2H), 3.95 (m, 4H), 3.55 (s, 2H), 3.2 (s, 6H), 2.85 (m, 2H), 2.15 (m, 2H), 1.40 (m, 2H), 1.15 (m, 2H). ESMS *m/z*: 483 (M + H)⁺.

*1-(2-Ethoxyethyl)-1*H*-imidazole-2-carbaldehyde (3A)*. Following the same procedure as utilized in the preparation of **2A**, the target compound was prepared from 1-bromo-2-ethoxyethane (3.51 g, 22 mmol) and imidazole-2-carboxaldehyde to yield the desired compound (580 mg, 3.56 mmol, 17% yield). ¹H NMR (400 MHz, DMSO-*d*₆) δ 9.63 (s, H), 7.6 (s, H), 7.21 (s, H), 4.45 (dd, 2H), 3.62 (dd, 2H), 3.38 (m, 2H), 1.05 (t, 3H).

*(S)-2-Amino-6-(bis((1-(2-ethoxyethyl)-1*H*-imidazol-2-yl)methyl)amino)hexanoic Acid (3)*. Following the same procedure as utilized in the preparation of **1** yielded the desired Fmoc-protected product (141 mg, 0.210 mmol, 44% yield). ¹H NMR (400 MHz, DMSO-*d*₆) δ 7.67 (d, 2H), 7.35 (m, 4H), 7.30 (m, 2H), 7.05 (s, H), 6.75 (s, H), 3.95 (m, 4H), 3.58 (d, 4H), 3.55 (s, 4H), 3.3 (s, 4H), 2.30 (m, 2H), 2.15 (m, 2H), 1.50 (m, 2H), 1.15 (s, 2H), 1.05 (t, 6H). ESMS *m/z*: 674 (M + H)⁺. The purified compound was deprotected by treatment with piperidine/DMF 1:1 (1 mL), and the mixture was stirred at room temperature for 18 h. Following evaporation to residue, aqueous extraction from DCM afforded the desired product (31 mg, 0.069 mmol, 91% yield) as an off-white solid. ¹H NMR (400 MHz, DMSO-*d*₆) δ 8.35 (s, H), 7.98 (s, H), 7.05 (s, H), 6.75 (s, H), 3.95 (m, 4H), 3.58 (d, 4H), 3.55 (s, 4H), 3.3 (s, 4H), 2.30 (m, 2H), 2.15 (m, 2H), 1.50 (m, 2H), 1.15 (s, 2H), 1.05 (t, 6H). ESMS *m/z*: 451 (M + H)⁺.

*tert-Butyl 2-(2-Formyl-1*H*-imidazol-1-yl)acetate (4A)*. Following the same procedure as utilized in the preparation of **2A**, the target compound was prepared from *tert*-butyl 2-bromoacetate and imidazole-2-carboxaldehyde to yield the desired compound (850 mg, 4.03 mmol, 39% yield). ¹H NMR (400 MHz, DMSO-*d*₆) δ 7.6 (s, H), 7.23 (s, H), 5.15 (s, 2H), 1.40 (s, 9H).

*(S)-2,2'-(2,2'-(5-Amino-5-carboxypentylazanediyl)bis(methylene)bis(1*H*-imidazole-2,1-diyl))diacetic Acid (4)*. Following the same procedure as utilized in the preparation of **1** yielded the desired Fmoc-protected product (155 mg, 0.205 mmol, 42% yield). ¹H

NMR (400 MHz, DMSO-*d*₆) δ 7.67 (d, 2H), 7.35 (m, 4H), 7.30 (m, 2H), 7.05 (s, H), 6.7 (s, H), 4.70 (s, 4H), 4.2 (m, 4H), 3.4 (d, 2H), 2.4 (m, 2H), 1.8 (s, 2H), 1.39 (s, 18H), 1.2 (m, 2H). ESMS *m/z*: 758 (M + H)⁺. The purified compound was deprotected by treatment with piperidine/DMF 1:1 (1 mL), and the mixture was stirred at room temperature for 18 h. Following evaporation to a residue, aqueous extraction from DCM afforded the desired product (25 mg, 0.047 mmol, 25% yield) as an off-white solid. ¹H NMR (400 MHz, DMSO-*d*₆) δ 7.0 (s, 2H), 6.65 (s, H), 4.70 (s, 4H), 4.2 (m, 4H), 3.2 (d, 2H), 2.4 (m, 2H), 1.8 (s, 2H), 1.39 (s, 18H), 1.15 (m, 2H). ESMS *m/z*: 535 (M + H)⁺.

*(S)-2-Amino-6-(bis((1-(2-hydroxyethyl)-1*H*-imidazol-2-yl)methyl)amino)hexanoic Acid (5)*. To a solution of **3** (25 mg, 0.055 mmol) dissolved in DCM (10 mL) was added 1.0 M boron tribromide in DCM (83 mg, 0.333 mmol) at –20 °C. The mixture was stirred at –20 °C for 2 h and was subsequently quenched with water and washed with excess DCM. The water portion was evaporated to dryness and purified as the product utilizing a Biotage SP4 with a gradient method of 5–50% methanol in DCM (15 mg, 0.038 mmol, 34% yield). ¹H NMR (400 MHz, DMSO-*d*₆) δ 8.40 (m, 2H), 8.16 (d, 2H), 7.70 (d, 2H), 5.50 (s, 2H), 4.20 (s, 2H), 4.05 (m, 4H), 3.68 (d, 2H), 3.15 (m, 5H), 2.46 (s, 2H), 1.70 (m, 2H), 1.65 (m, 2H), 1.21 (m, 2H). ESMS *m/z*: 395 (M + H)⁺.

*Diethyl 3-(2-Formyl-1*H*-imidazol-1-yl)propylphosphonate (6A)*. Following the same procedure as utilized in the preparation of **2A**, the target compound was prepared from diethyl (3-bromopropyl)phosphonate (2.96 g, 11.4 mmol) and imidazole-2-carboxaldehyde to yield the desired compound (466 mg, 1.69 mmol, 16% yield). ESMS *m/z*: 275 (M + H)⁺.

*(S)-2-Amino-6-(bis((1-(3-(diethoxyphosphoryl)propyl)-1*H*-imidazol-2-yl)methyl)amino)hexanoic Acid (6)*. Following the same procedure as utilized in the preparation of **1** yielded the desired Fmoc-protected product (63 mg, 0.071 mmol, 21% yield). ESMS *m/z*: 443 (M/2). The purified compound (53 mg, 0.060 mmol) was deprotected by treatment with piperidine/DMF 1:1 (1 mL), and the mixture was stirred at room temperature for 18 h. Following evaporation to a residue, aqueous extraction from DCM afforded the desired product (32 mg, 0.048 mmol, 80% yield) as an off-white solid. ¹H NMR (400 MHz, DMSO-*d*₆) δ 7.1 (s, 2H), 6.78 (s, 2H), 3.98 (m, 4H), 3.8 (m, 4H), 3.6 (s, 4H), 2.85 (m, 4H), 2.75 (s, H), 2.38 (s, 2H), 1.77 (m, 4H), 1.55 (m, 4H), 1.39 (s, 2H), 1.18 (t, 12H). ESMS *m/z*: 664 (M + H)⁺.

(S)-2-Amino-6-((carboxymethyl)(thiazol-2-ylmethyl)amino)hexanoic Acid (7). A suspension of Fmoc-Lys-OH·HCl (6.1 g, 15 mmol) and thiazole-2-carbaldehyde (1.697 g, 15 mmol) in DCE (100 mL) was refluxed for 30 min under nitrogen. The reaction mixture was cooled to 0 °C and treated sequentially with sodium triacetoxycyborohydride (7.9 g, 38 mmol) and crude *tert*-butyl glyoxalate (3.53 g, 27 mmol) as previously reported (26). The reaction mixture was stirred at room temperature overnight and decomposed with water. The reaction mixture was extracted with DCM. The organic layer was dried and concentrated under reduced pressure. The residue was purified by flash chromatography over silica gel to afford (S)-1-(9*H*-fluoren-9-yl)-14,14-dimethyl-3,12-dioxo-10-(thiazol-2-ylmethyl)-2,13-dioxo-4,10-diazapentadecane-5-carboxylic acid (1.85 g, 21%). MS (ESI), 580 (M + H)⁺. To a solution of (S)-1-(9*H*-fluoren-9-yl)-14,14-dimethyl-3,12-dioxo-10-(thiazol-2-ylmethyl)-2,13-dioxo-4,10-diazapentadecane-5-carboxylic acid (72.5 mg, 0.125 mmol) in DMF (1.0 mL) was added piperidine (0.20 mL). The mixture was stirred at room temperature for 2 h. Solvent was evaporated under reduced pressure to afford a residue, which was purified by flash chromatography over silica eluting with 10% MeOH in DCM to afford (S)-2-amino-6-((2-*tert*-butoxy-2-oxoethyl)(thi-

azol-2-ylmethyl)amino)hexanoic acid (25 mg, 0.083 mmol, 66%). ^1H NMR (400 MHz, CD_3OD) δ 7.70 (d, $J = 3.6$ Hz, 1 H), 7.52 (d, $J = 3.6$ Hz, 1 H), 4.15 (s, 2 H), 3.52 (dd, $J = 7.2$, 5.2 Hz, 1 H), 3.39 (s, 2 H), 2.73 (t, $J = 7.2$ Hz, 2 H), 1.91–1.76 (m, 2 H), 1.60–1.57 (m, 2 H), 1.55–1.47 (m, 11 H). MS (ESI): 358 (M + H) $^+$.

(*S*)-2-Amino-6-((2-*tert*-butoxy-2-oxoethyl)((1-methyl-1*H*-imidazol-2-yl)methyl)amino)hexanoic Acid (**8**). The title compound was prepared by following the same procedure as described in the preparation of **7** except 1-methyl-1*H*-imidazole-2-carbaldehyde was used in place of thiazole-2-carbaldehyde. ^1H NMR (400 MHz, CDCl_3) δ 7.88 (d, $J = 7.2$ Hz, 2 H), 7.71 (dd, $J = 7.2$, 2.4 Hz, 2 H), 7.55 (d, $J = 8.0$ Hz, 1 H), 7.40 (t, $J = 7.6$ Hz, 2 H), 7.31 (t, $J = 7.6$ Hz, 4 H), 7.01 (s, 1 H), 6.71 (s, 1 H), 4.27–4.18 (m, 3 H), 3.88–3.83 (m, 1 H), 3.72 (s, 2 H), 3.14 (s, 2 H), 1.62–1.50 (m, 2 H), 1.38 (s, 9 H), 1.33–1.21 (m, 4 H). MS (ESI): 577 (M + H) $^+$. To a solution of (*S*)-1-(9*H*-fluoren-9-yl)-14,14-dimethyl-10-((1-methyl-1*H*-imidazol-2-yl)methyl)-3,12-dioxo-2,13-dioxo-4,10-diazapentadecane-5-carboxylic acid (190 mg, 0.33 mmol) in DMF (2 mL) was added piperidine (0.4 mL). The mixture was stirred at room temperature for 2 h. Solvent was evaporated under reduce pressure to afford a residue, which was purified by Amberchrom column chromatography to afford (*S*)-2-amino-6-((2-*tert*-butoxy-2-oxoethyl)((1-methyl-1*H*-imidazol-2-yl)methyl)amino)hexanoic acid (115 mg, 0.32 mmol, 97%). ^1H NMR (400 MHz, DMSO) δ 7.27 (brs, 1 H), 7.04 (s, 1 H), 6.72 (s, 1 H), 3.73 (s, 2 H), 3.64 (s, 3 H), 3.15 (s, 2 H), 3.04 (dd, $J = 6.8$, 5.2 Hz, 1 H), 2.47 (t, $J = 7.2$ Hz, 2 H), 1.65–1.46 (m, 2 H), 1.39 (s, 9 H), 1.30–1.21 (m, 4 H). MS (ESI): 355 (M + H) $^+$.

(*S*)-2,2'-(5-Amino-5-carboxypentylazanediy)diacetic Acid (**9**). (*S*)-10-(2-*tert*-Butoxy-2-oxoethyl)-1-(9*H*-fluoren-9-yl)-14,14-dimethyl-3,12-dioxo-2,13-dioxo-4,10-diazapentadecane-5-carboxylic acid was prepared from a solution of Fmoc-Lys-OH (1.5 g, 4.0 mmol) and crude *tert*-butyl glyoxalate (3.6 g, 27.6 mmol) in DCE (50 mL), and the mixture was stirred at 75 °C for 30 min under nitrogen. The reaction mixture was cooled to 0 °C and treated with sodium triacetoxyborohydride (2.1 g, 10 mmol). The reaction mixture was stirred at room temperature for 3 h and decomposed with water. The reaction mixture was extracted with DCM. The organic layer was dried and concentrated under reduced pressure. The residue was purified by flash chromatography over silica gel to afford (*S*)-10-(2-*tert*-butoxy-2-oxoethyl)-1-(9*H*-fluoren-9-yl)-14,14-dimethyl-3,12-dioxo-2,13-dioxo-4,10-diazapentadecane-5-carboxylic acid (1.70 g, 3.51 mmol 71%). ^1H NMR (400 MHz, CDCl_3) δ 7.76 (d, $J = 7.2$ Hz, 2 H), 7.60 (d, $J = 7.2$ Hz, 2 H), 7.40 (t, $J = 7.2$ Hz, 2 H), 7.30 (t, $J = 7.2$ Hz, 2 H), 6.63 (d, $J = 7.6$ Hz, 1 H), 4.40–4.34 (m, 3 H), 4.22 (t, $J = 7.2$ Hz, 1 H), 3.49 (s, 4 H), 2.83–2.64 (m, 4 H), 1.96–1.77 (m, 4 H), 1.40 (s, 18 H). MS (ESI): 598 (M + H) $^+$. The purified compound (12 mg, 0.21 mmol) was deprotected by treatment with piperidine/DMF 1:1 (1 mL), and the mixture was stirred at room temperature for 18 h. Following evaporation to a residue, aqueous extraction from DCM afforded the desired product **9** (3 mg, 0.11 mmol, 55% yield) as an off-white solid. ^1H NMR (400 MHz, DMSO- d_6) δ 7.9 (s, 2H), 3.5 (m, H), 3.3 (d, 2H), 2.4 (m, 2H), 1.8 (s, 2H), 1.45 (m, 2H), 1.15 (m, 2H). ESMS m/z : 263 (M + H) $^+$.

General Preparation of ^{99m}Tc Complexes and Peptides. The $^{99m}\text{Tc}(\text{I})(\text{CO})_3^+$ radiolabeling of the SAAC systems to form the metal complexes was accomplished on either the free α -amino acids or the α -*N*-Fmoc protected lysine derivative utilizing similar methodology. The radiolabeling was accomplished in two steps using commercially available IsoLink kits (Covidien) to form the $[\text{C}^{99m}\text{Tc}(\text{CO})_3(\text{H}_2\text{O})_3]^+$ intermediate, which was neutralized and reacted with the appropriate SAAC system (Figure 2) at 10^{-6} – 10^{-4} M in an equal volume mixture of

acetonitrile and water in a sealed vial. The sealed vial was heated at 100 °C for 30 min, and upon cooling, the mixture was analyzed for purity via reverse-phase HPLC. Purification by HPLC resulted in “carrier-free” products, and the RCP was determined via HPLC and shown to be consistently $\geq 95\%$ pure. The radiolabeling can be achieved at concentrations as low as 10^{-6} M at 75 °C with RCY $\leq 80\%$ and with RCY $> 95\%$ when conducted at 10^{-4} M at 75 °C.

The $^{99m}\text{Tc}(\text{I})(\text{CO})_3^+$ radiolabeling of the SAAC-conjugated peptides was achieved and purified in a similar manner with the exception of the heating temperature, which was reduced to 60 °C. The ^{111}In -DOTA-Tyr-3-octreotide was prepared from $^{111}\text{InCl}_3$ in an aqueous solution (10^{-4} M of the peptide) by heating at 100 °C for 30 min.

Determination of log *P* Values. The log *P* values of the $^{99m}\text{Tc}(\text{I})$ complexes were determined using the following procedure: The ^{99m}Tc radiotracer was prepared and purified by reverse-phase HPLC. The collected mobile phase was evaporated and the residue dissolved in an equal volume mixture of *n*-octanol and 25 mM phosphate buffer (pH 7.4). The samples were extracted as follows: the samples were vortexed for 20 min and centrifuged at 8000 rpm for 5 min, and then aliquots were removed from both the aqueous phosphate buffer and the organic *n*-octanol layers and counted separately in a γ counter (LKB model 1282, Wallac Oy, Finland). The extraction was repeated twice for a total number of three extractions to ensure full extraction of all the organic components. The partition coefficients were then calculated using the equation $P = (\text{activity concentration in } n\text{-octanol})/(\text{activity concentration in aqueous layer})$. The samples were analyzed in triplicate and the log *P* values determined from the average of the three different measurements.

Rat Tissue Distribution of SAAC Complexes. Tissue distribution studies of the ^{99m}Tc SAAC systems were performed in separate groups of male Sprague–Dawley rats ($n = 5/\text{time point}$) administered as a bolus intravenous injection (approximately 10 $\mu\text{Ci}/\text{rat}$) in a constant volume of 0.1 mL. Animals were euthanized by carbon dioxide at 5, 30, 60, and 120 min after injection. Blood, heart, lungs, liver, spleen, kidneys, adrenals, stomach (with contents), large and small intestines (with contents), testes, skeletal muscle, bone, brain, and adipose were excised, weighed wet, transferred to plastic tubes, and counted in an automated γ counter (LKB model 1282, Wallac Oy, Finland). Aliquots of the injected dose were also measured to convert the counts per minute in each tissue sample to percent-injected dose per organ. Tissue radioactivity levels, expressed as %ID/g, were determined by converting the decay corrected counts per minute to the percent dose and dividing by the weight of the tissue or organ sample.

Peptide Synthesis. Tyr-3-octreotide analogues {4-Tyr-3-octreotide} and {DpK-Tyr-3-octreotide} with the lysine SAAC incorporated at the amino terminus were synthesized by AnaSpec, Inc. (San Jose, CA) using solid phase peptide synthesis employing standard Fmoc coupling techniques with cleavage and deprotection using TFA. Following synthesis, all peptides were purified using reverse phase HPLC and were lyophilized with purity profiles of $>90\%$.

Tumor Cell Lines. AR42J cells were obtained from American Type Culture Collection (Rockville, MD). The cells were grown in Kaighn's F-12 media supplemented with 20% fetal bovine serum, sodium pyruvate, and gentamicin in a humidified atmosphere of 5% $\text{CO}_2/95\%$ air at 37 °C.

Tissue Distribution in AR42J Bearing Mice. Uptake of radiolabeled peptides in rat tumor xenograft models were performed according to published methods. Briefly, AR42J cells were trypsinized, counted, and suspended in a solution containing 50% Dulbecco's PBS (D-PBS) (with 1 mg/mL D-glucose

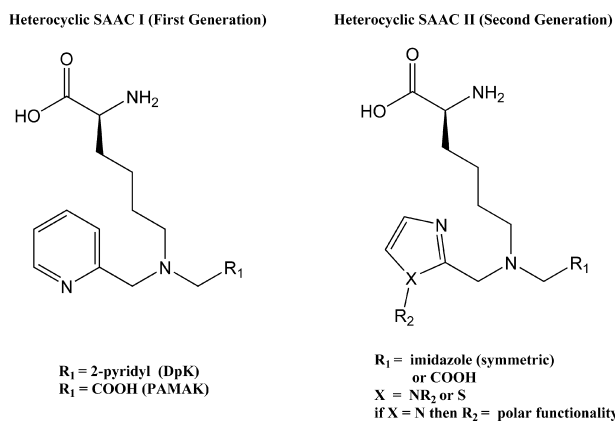


Figure 1. General structures of the first and second generation of heterocyclic SAAC systems.

and 36 $\mu\text{g/mL}$ sodium pyruvate) and 50% Matrigel (BD Biosciences, Franklin Lakes, NJ). Male $\text{NCR}^{\text{nu/nu}}$ mice were anesthetized by intraperitoneal injection of 0.5 mL of Avertin (20 mg/mL) (Sigma-Aldrich, St. Louis, MO) and then inoculated subcutaneously into the hind flank with 2×10^6 cells in a 0.25 mL suspension volume. Studies of tumor uptake were conducted when the tumors reached a size of 600–800 mm^3 . Tissue biodistribution studies were conducted by administering, via the tail vein, a bolus injection of 2 $\mu\text{Ci}/\text{mouse}$ in a constant volume of 0.05 mL of D-PBS containing 1 mg/mL bovine serum albumin. Groups of five animals were euthanized by asphyxiation with carbon dioxide at 1 and 4 h after injection. All tissues from Figure 4, including the tumor, were excised, weighed wet, and transferred to plastic tubes, and radioactivity present was counted in an automated γ -counter (LKB model 1282, Wallac Oy, Finland). Tissue time – radioactivity levels were expressed as % injected dose per gram tissue (%ID/g).

RESULTS AND DISCUSSION

We previously described a technology known as SAAC, a radiolabeling platform that has broad utility in radiochemical, fluorescent, and dual modality (radio/fluorescent) molecular imaging (6, 9) and is particularly convenient for developing radiolabeled peptides. One limitation of the $\text{Tc}(\text{CO})_3$ -dipyridyl complex, characteristic of the original SAAC systems, is the extremely hydrophobic nature of the radiolabeled complexes which has often led to the liver accumulation and/or hepatobiliary clearance of the bioconjugates. This undesirable pharmacokinetic profile is not unique to the original SAAC systems but a characteristic shared by many bioconjugates (27, 28). The goal of this work was to develop a second generation series of hydrophilic lysine-based SAAC systems that have been modified to favor renal clearance of the $^{99\text{m}}\text{Tc}$ -SAAC complexes and thus facilitate the development of novel $^{99\text{m}}\text{Tc}$ -labeled radiopharmaceuticals that clear the body more readily. This was accomplished, as shown in Figure 1, by modifying the lysine core of SAAC systems in two ways to create novel tridentate chelators with reduced lipophilicity: the addition of polar substituents and the reduction of the ligand size. The N-protected lysine building block of the SAAC systems was derivatized at the ϵ amine with substituted heterocyclic rings (R_1) that contained distinct polar functional groups (R_2) in an attempt to reduce the lipophilicity of the resulting $^{99\text{m}}\text{Tc}$ complexes. The ϵ amine of lysine allows for the facile synthesis of large numbers of structural variants of SAAC systems with the potential of diverse physiochemical properties. The chemical synthesis of the bifunctional SAAC systems was accomplished via reductive alkylation of N-Fmoc protected lysine with the appropriate heterocyclic aldehyde. The availability of a diverse set of

heterocyclic aldehydes coupled with the ease of synthesis has led to the preparation of several classes of polar SAAC systems that form cationic $^{99\text{m}}\text{Tc}$ complexes with enhanced renal clearance. In addition, incorporation of one acetic acid “arm” onto the ϵ amine of lysine (R_1) in lieu of the second heterocyclic ligand affords SAAC systems of reduced size with a neutral metal center.

Ligand Design. As illustrated in Figure 1, both first generation (SAAC I) and second generation (SAAC II) SAAC systems were derived from the amino acid lysine. First generation ligands incorporated either two pyridine rings or a pyridine and an acetic acid for R_1 . The design of the novel second generation bifunctional chelates explored the concept of increasing the water solubility of the chelate ring systems through the modification of heterocyclic imidazole ring substituents for R_2 . The effort focused on the SAAC ligands that form cationic homogeneous tridentate metal complexes as well as the smaller heterogeneous monoacetic acid derivatized compounds which form neutral metal complexes.

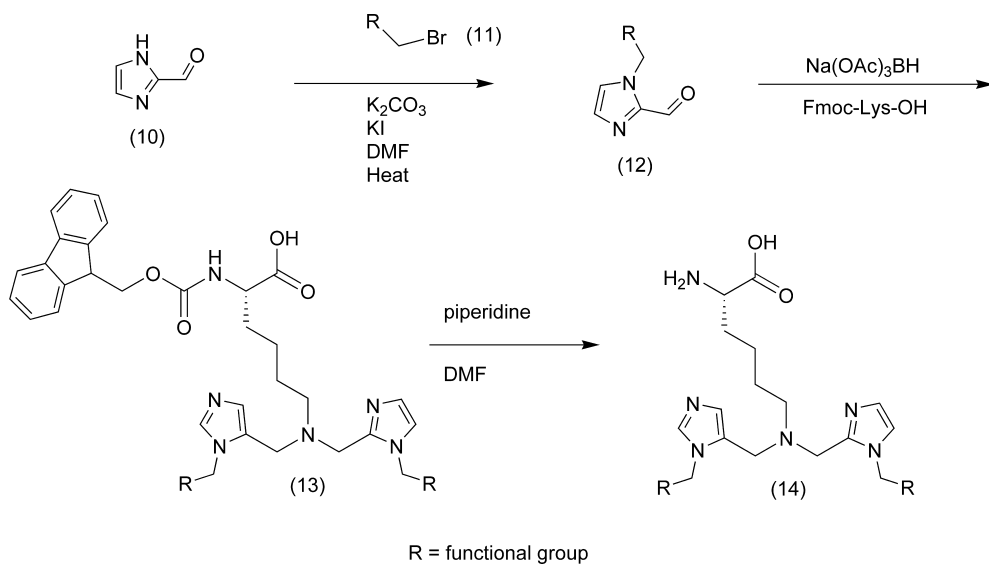
Preparation of Homogeneous Tridentate Ligands as Second Generation Lysine Imidazole Derivatized SAAC Systems. The derivatized imidazole SAAC systems were prepared via the alkylation of the commercially available imidazole-2-carboxaldehyde (10) with the desired alkyl halide (11) to afford the N-substituted imidazole-2-carboxaldehyde analogues (12). Reductive amination of N-Fmoc lysine with sodium triacetoxyborohydride produces the N-Fmoc protected SAAC system (13) which following deprotection with piperidine affords the desired SAAC systems (14) in good yields as illustrated in Scheme 1.

Preparation of Heterogeneous SAAC Systems: Monoacetic Acid Analogues. Several compounds from the homogeneous series described above which exhibited promising pharmacokinetic profiles were prepared as their corresponding monoacetic acid analogues, shown in Figure 2. These new heterogeneous $^{99\text{m}}\text{Tc}$ -SAAC complexes were smaller in size, were less hindered complexes, and were uncharged at the metal center, in contrast to the positive charged metal centers of the homogeneous complexes.

The compounds in this series were prepared using the double reductive alkylation sequence on Fmoc-lysine. Addition of the first aldehyde followed by reduction with sodium borohydride affords a monoalkylated intermediate as shown in Scheme 2. Subsequent treatment with *tert*-butyl glyoxalate followed by deprotections with piperidine and trifluoroacetic acid (TFA) afforded the desired series of heterogeneous neutral ligands (26).

Radiolabeling of $^{99\text{m}}\text{Tc}$ -SAAC. Radiolabeling of the SAAC systems was accomplished on either the free α -amino acids or as the appropriately N-protected amino acid derivative utilizing similar methodology to form $^{99\text{m}}\text{Tc}$ -1–9, demonstrating the flexibility of the radiolabeling and the ease of preparation of these novel SAAC metal complexes. The $^{99\text{m}}\text{Tc}(\text{I})(\text{CO})_3^+$ radiolabeling was accomplished in two steps using the commercially available IsoLink kits (Covidien) to form the $[\text{^{99m}Tc}(\text{CO})_3(\text{H}_2\text{O})_3]^+$ intermediate, which was reacted with the appropriate SAAC ligand (ligand concentration of 10^{-6} – 10^{-4} M) in an equal volume mixture of 1:1 acetonitrile and phosphate buffer. The sealed vial was heated at 100 $^\circ\text{C}$ for 30 min, and upon cooling, the mixture was analyzed for purity via HPLC. The RCP after HPLC purification resulted in “carrier-free” products, with purity determined via HPLC to be consistently $\geq 95\%$. While possible to radiolabel at concentrations as low as 10^{-6} M, the RCY at 75 $^\circ\text{C}$ was $\leq 80\%$. To achieve RCY > 95% at 75 $^\circ\text{C}$, the ligand concentration needed to be increased to 10^{-4} M. This was true for all of the compounds with the exception of 2,2'-(5-amino-5-carboxypentylazanediyldiacetic acid (9) which required 10^{-3} M ligand to achieve >95% RCY.

Scheme 1. Preparation of Homogeneous Bifunctional Imidazole SAAC Systems



SAAC systems 2,2'-(2,2'-(5-amino-5-carboxypentylazanediyl)-bis(methylene)-bis(1*H*-imidazole-2,1-diyl)diacetic acid (4) and

2-amino-6-(bis((1-(2-hydroxyethyl)-1*H*-imidazol-2-yl)methyl)-amino)hexanoic acid (5) could be radiolabeled with the ester

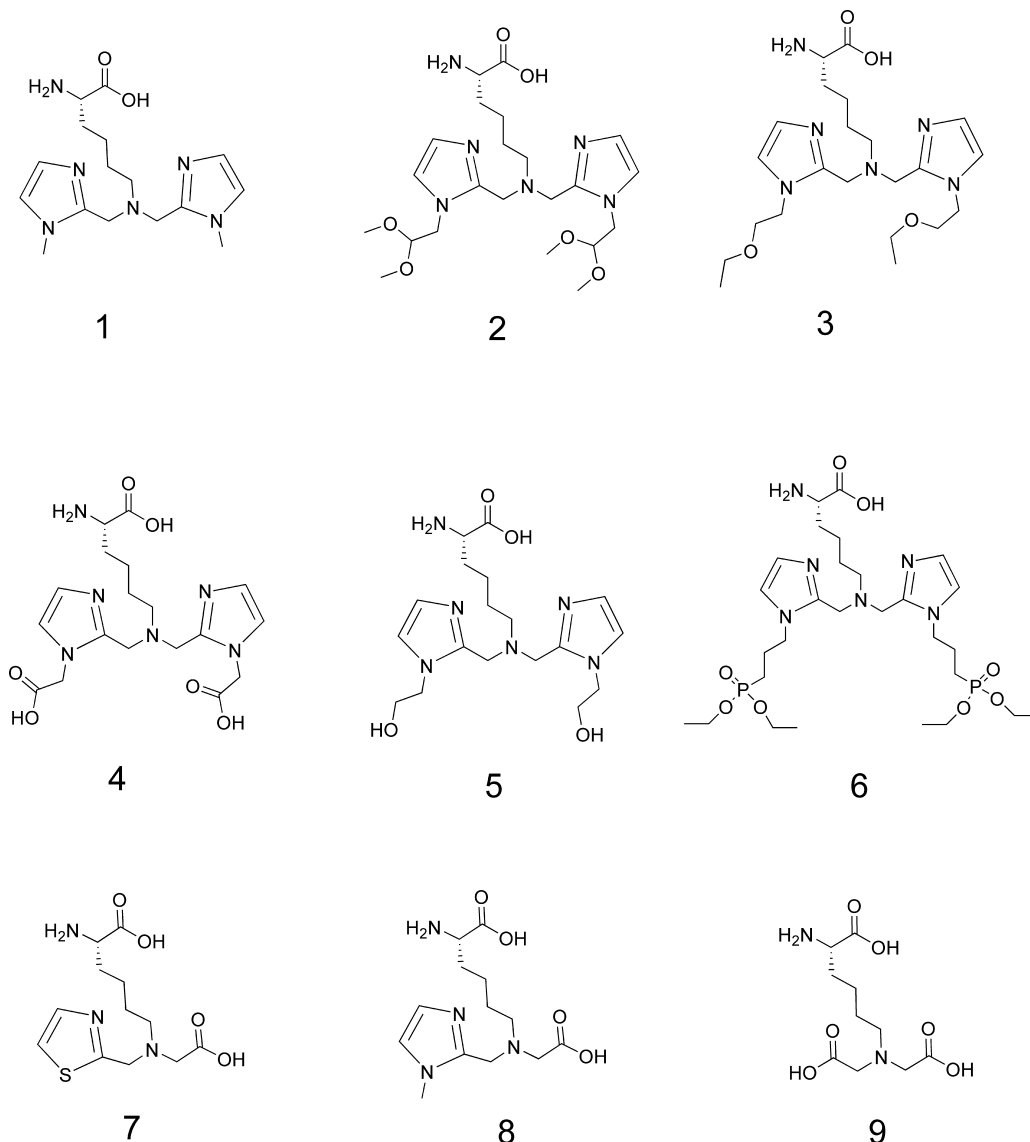
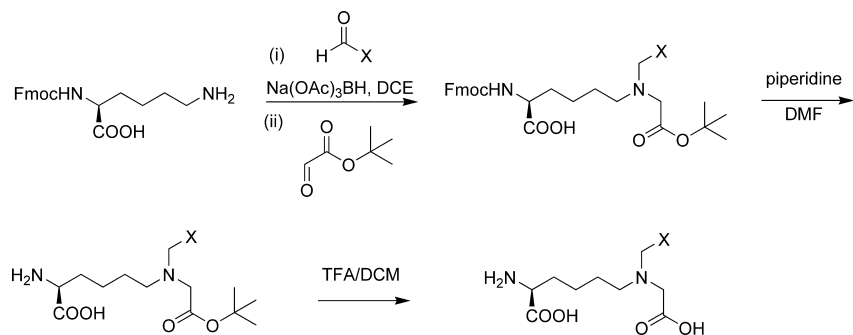


Figure 2. Structures of the novel lysine based SAAC systems.

Scheme 2. Preparation of the Heterogeneous SAAC Systems



protecting groups present on the bis-imidazole derivative or on the fully deprotected ligand. For example, the ^{99m}Tc complex of ligand **4** was prepared in 30 min followed by simple deprotection of the *tert*-butyl ester protecting groups using TFA at room temperature to produce ^{99m}Tc -**4**. The radiolabeling and subsequent deprotection could be followed by HPLC over time, as shown in Figure 3.

The ^{99m}Tc complex of 2-amino-6-(bis((1-(2-hydroxyethyl)-1*H*-imidazol-2-yl)methyl)amino)hexanoic acid (**5**) could be prepared by radiolabeling 2-amino-6-(bis((1-(2-ethoxyethyl)-1*H*-imidazol-2-yl)methyl)amino)hexanoic acid (**3**) followed by subsequent deprotection of the ethyl ethers using BBr_3 to afford the desired metal complex ^{99m}Tc -**5** (Scheme 3). Confirmation of the formation of the ^{99m}Tc -**5** complex was established by

independent radiolabeling studies of the compounds **3** and **5** followed by the radiolabeling of **3** with conversion to the ^{99m}Tc -**5** complex.

Rat Tissue Distribution Studies of SAAC Complexes. Rat tissue distribution studies were performed with eight of the novel SAAC complexes, [$^{99m}\text{Tc}(\text{CO})_3\{\eta^3\text{-}((S)\text{-}2\text{-amino-6-(bis}((1\text{-methyl-1*H*-imidazol-2-yl)methyl)amino)hexanoic acid})\}$] (^{99m}Tc -**1**), [$^{99m}\text{Tc}(\text{CO})_3\{\eta^3\text{-}(2\text{-amino-6-(bis}((1\text{-}(2,2\text{-dimethoxyethyl)-1*H*-imidazol-2-yl)methyl)amino)hexanoic acid})\}$] (^{99m}Tc -**2**), [$^{99m}\text{Tc}(\text{CO})_3\{\eta^3\text{-}(2\text{-amino-6-(bis}((1\text{-}(2\text{-ethoxyethyl)-1*H*-imidazol-2-yl)methyl)amino)hexanoic acid})\}$] (^{99m}Tc -**3**), [$^{99m}\text{Tc}(\text{CO})_3\{\eta^3\text{-}(2,2'\text{-}(2,2'\text{-}(5\text{-amino-5-carboxypentylazanediy)bis(methylene)-bis(1*H*-imidazole-2,1-diyl)diacetic acid})\}$] (^{99m}Tc -**4**), [$^{99m}\text{Tc}(\text{CO})_3\{\eta^3\text{-}(2\text{-amino-6-(bis}((1\text{-}(2\text{-hydroxyethyl)-1*H*-imidazol-$

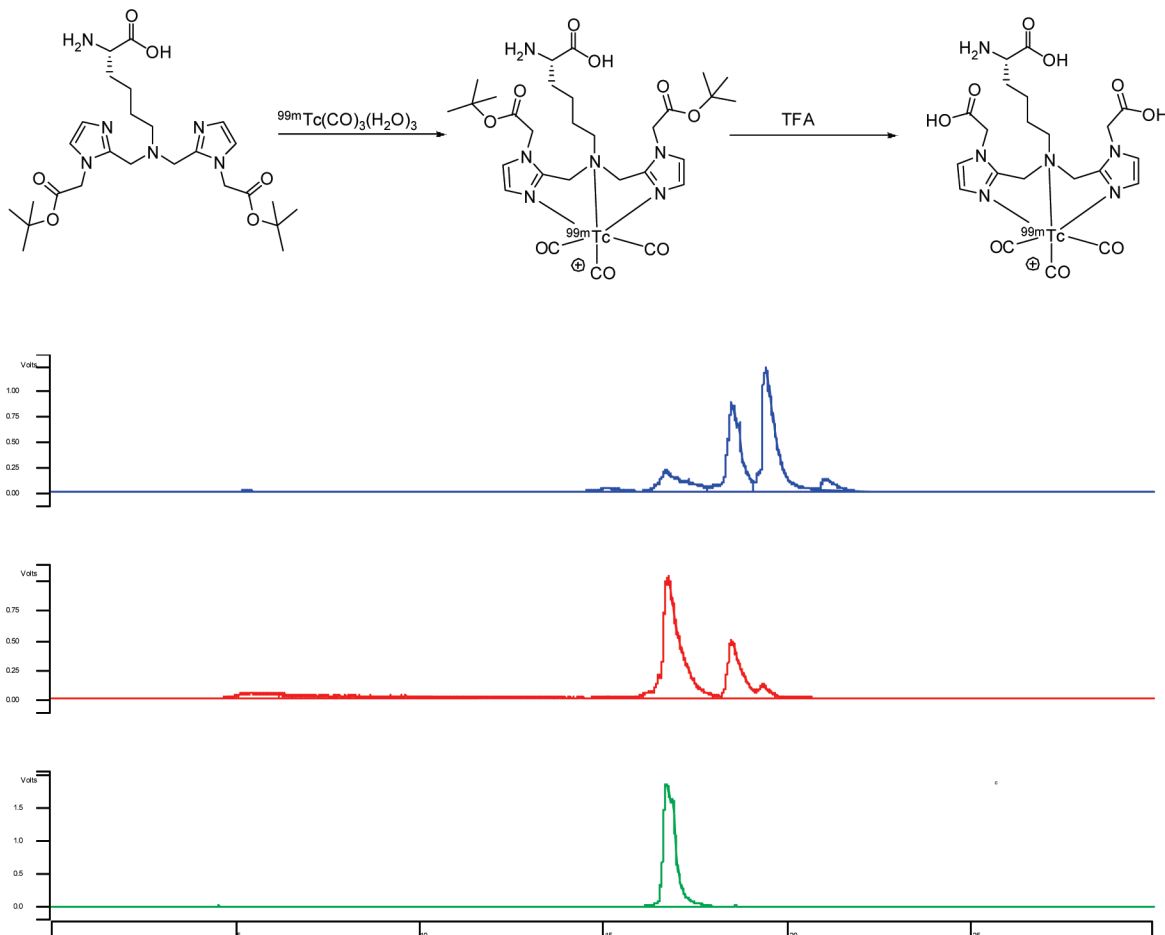
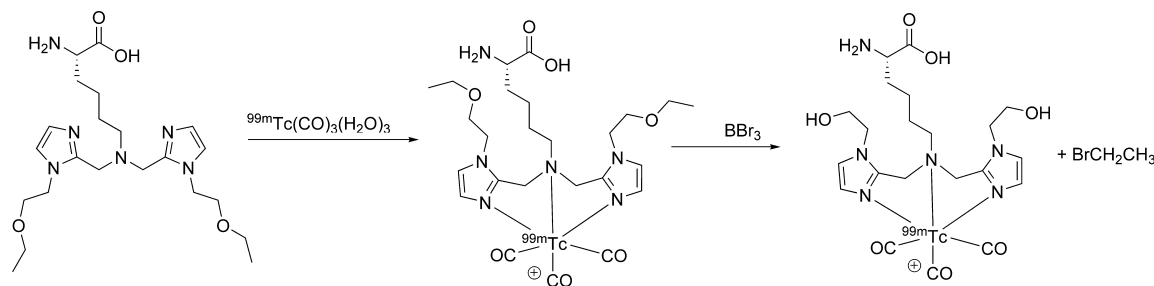


Figure 3. Radiochromatograms of ^{99m}Tc -**4**-di-*tert*-butyl ester: crude reaction after heating at 75 °C for 30 min (blue) showing multiple radioactive species; after TFA incubation (red) showing predominantly fully deprotected product (^{99m}Tc -**4**); after reverse phase HPLC purification (green) demonstrating ^{99m}Tc -**4** > 98% RCP.

Scheme 3. Radiolabeling of (2-Amino-6-(bis((1-(2-ethoxyethyl)-1H-imidazol-2-yl)methyl)amino)hexanoic acid (3) and Subsequent Deprotection To Form the Metal Complex ^{99m}Tc -5



2-yl)methyl)amino)hexanoic acid)] (^{99m}Tc -5), [$^{99m}\text{Tc}(\text{CO})_3\{\eta^3\text{-}((S)\text{-}2\text{-amino-}6\text{-}((\text{carboxymethyl})(\text{thiazol-}2\text{-ylmethyl)amino)hexanoic acid } (^{99m}\text{Tc}\text{-}7), [^{99m}\text{Tc}(\text{CO})_3\{\eta^3\text{-}((S)\text{-}2\text{-amino-}6\text{-}((2\text{-tert-butoxy-}2\text{-oxoethyl})((1\text{-methyl-}1H\text{-imidazol-}2\text{-yl)methyl)amino)hexanoic acid } (^{99m}\text{Tc}\text{-}8), \text{ and } [^{99m}\text{Tc}(\text{CO})_3\{\eta^3\text{-}(2,2'\text{-}(5\text{-amino-}5\text{-carboxypentylazanediy)diacetic acid)}\} (^{99m}\text{Tc}\text{-}9)$. Only [$^{99m}\text{Tc}(\text{CO})_3\{\eta^3\text{-}(2\text{-amino-}6\text{-}(\text{bis}((1\text{-}(3\text{-}(\text{diethoxyphosphoryl)propyl})\text{-}1H\text{-imidazol-}2\text{-yl)methyl)amino)hexanoic acid)}\} (^{99m}\text{Tc}\text{-}6)$ was omitted because of the high lipophilicity of the complex. In addition, for comparison, rat tissue distribution studies were performed with previously published SAAC systems (6), the cationic bis-pyridine complex [$^{99m}\text{Tc}(\text{CO})_3(\eta^3\text{-}\{2\text{-amino-}6\text{-}(\text{bis}(\text{pyridin-}2\text{-ylmethyl)amino)hexanoic acid}\}) [^{99m}\text{Tc}\text{-DpK}]$ and the neutral pyridine amine monoacetic acid complex [$^{99m}\text{Tc}(\text{CO})_3(\eta^3\text{-}\{2\text{-amino-}6\text{-}((\text{carboxymethyl})(\text{pyridin-}2\text{-ylmethyl)amino)hexanoic acid}\}) [^{99m}\text{Tc}\text{-PAMAK}]$. A summary of the uptake of all of the SAAC complexes examined in selected organs is shown in Table 1.

^{99m}Tc -SAAC imidazole complexes **1**, **2**, **3**, and **5** exhibited rapid clearance from the blood (maximum of 0.14 %ID/g at 2 h for ^{99m}Tc -5), relatively low liver uptake (maximum of 1.61 \pm 0.32 %ID/g at 5 min for ^{99m}Tc -3), and low liver retention (maximum of 0.74 \pm 0.14 %ID/g at 2 h for ^{99m}Tc -1). In addition, these complexes exhibited a shift from hepatobiliary clearance to a predominantly renal uptake pattern compared to ^{99m}Tc -DpK and ^{99m}Tc -PAMAK. However, the high renal accumulation was in the absence of substantial renal clearance over the 2 h time period of the study. The four complexes displayed >12 %ID/g in the kidneys at the earliest (0.5 h) and latest (2 h) time points tested, demonstrating very little clearance over time. It is not clear whether the undesirable kidney retention was due to nonspecific binding of the complexes in the kidneys or a result of amino acid recycling. Since the goal is to develop chelators that exhibit rapid clearance from all nontarget tissues, the extended retention in the kidneys can be viewed as a significant liability for the complexes and may mitigate their potential application to biologically relevant molecules.

^{99m}Tc -SAAC complex **4**, which contains carboxylic acid functionalized imidazole rings, also exhibited very low liver and gastrointestinal accumulation (0.39 \pm 0.07 and 1.22 \pm 0.27 %ID/g at 2 h) and high kidney uptake that did not clear over the time course of the study (10.7 \pm 2.3 and 10.2 \pm 2.5 %ID/g at 0.5 and 2 h, respectively). This complex exhibited the least initial liver uptake (0.52 \pm 0.07 %ID/g at 5 min) of any chelate tested. Interestingly, **4** cleared the blood more slowly than any of the chelators examined, potentially because of increased binding to blood proteins.

The complexes of compounds **7** and **8**, the monothiazole and monomethylimidazole analogues, exhibited high kidney uptake, 9.07 \pm 0.66 and 17.05 \pm 3.17 %ID/g at 0.5 h, respectively, and rapid clearance of 1.63 \pm 0.51 and 3.94 \pm 0.43 %ID/g at 2 h, respectively. However, these complexes also demonstrated increased accumulation in the gastrointestinal tract (GI)

Table 1. Comparison of the Rat Tissue Distribution Results of ^{99m}Tc -SAAC Complexes in Blood and Excretory Tissues^a

compd	tissue	time (min)			
		5	30	60	120
DpK	blood	0.58 \pm 0.05	0.07 \pm 0.01	0.025 \pm 0.005	0.013 \pm 0.001
	liver	3.36 \pm 0.44	2.75 \pm 0.11	2.59 \pm 0.08	2.12 \pm 0.06
	kidney	6.05 \pm 1.03	4.95 \pm 0.11	4.93 \pm 0.43	3.89 \pm 0.42
	GI	0.49 \pm 0.08	0.89 \pm 0.07	1.46 \pm 0.09	2.73 \pm 0.57
PAMAK	blood	0.63 \pm 0.06	0.19 \pm 0.02	0.07 \pm 0.002	0.03 \pm 0.01
	liver	1.25 \pm 0.14	1.34 \pm 0.20	0.56 \pm 0.05	0.20 \pm 0.03
	kidney	6.38 \pm 0.70	3.55 \pm 0.35	1.14 \pm 0.14	0.48 \pm 0.05
	GI	0.18 \pm 0.02	1.22 \pm 0.24	1.80 \pm 0.175	2.50 \pm 0.59
1	blood	1.18 \pm 0.18	0.28 \pm 0.03	0.11 \pm 0.02	0.03 \pm 0.01
	liver	0.8 \pm 0.28	1.03 \pm 0.21	0.86 \pm 0.16	0.74 \pm 0.14
	kidney	6.65 \pm 2.06	22.2 \pm 0.39	25.4 \pm 1.7	25.5 \pm 3.4
	GI	0.15 \pm 0.02	0.45 \pm 0.11	0.84 \pm 0.1	1.12 \pm 0.37
2	blood	1.46 \pm 0.21	0.47 \pm 0.05	0.14 \pm 0.04	0.04 \pm 0.01
	liver	1.06 \pm 0.34	0.45 \pm 0.04	0.24 \pm 0.04	0.16 \pm 0.02
	kidney	13.82 \pm 2.81	34.1 \pm 5.59	40.25 \pm 5.17	33.18 \pm 2.75
	GI	0.34 \pm 0.12	1.05 \pm 0.2	1.39 \pm 0.24	1.21 \pm 0.27
3	blood	0.83 \pm 0.09	0.09 \pm 0.02	0.002 \pm 0.001	0.01 \pm 0.001
	liver	1.61 \pm 0.32	0.35 \pm 0.08	0.28 \pm 0.07	0.14 \pm 0.02
	kidney	6.86 \pm 0.86	12.13 \pm 2.36	12.54 \pm 1.00	12.54 \pm 0.81
	GI	0.57 \pm 0.13	2.33 \pm 0.61	3.62 \pm 0.3	2.96 \pm 0.44
4	blood	1.33 \pm 0.2	1.14 \pm 0.23	0.86 \pm 0.17	0.72 \pm 0.12
	liver	0.52 \pm 0.07	0.55 \pm 0.07	0.42 \pm 0.08	0.39 \pm 0.07
	kidney	6.58 \pm 1.85	10.7 \pm 2.3	16.8 \pm 4.8	10.2 \pm 2.5
	GI	0.15 \pm 0.02	0.44 \pm 0.08	0.76 \pm 0.31	1.22 \pm 0.27
5	blood	1.3 \pm 0.25	0.52 \pm 0.03	0.24 \pm 0.03	0.14 \pm 0.02
	liver	0.88 \pm 0.24	0.95 \pm 0.13	0.65 \pm 0.13	0.46 \pm 0.14
	kidney	8.55 \pm 1.54	18.7 \pm 1.2	22.1 \pm 3.5	23.2 \pm 5.0
	GI	0.19 \pm 0.05	0.52 \pm 0.09	0.76 \pm 0.24	0.97 \pm 0.37
7	blood	0.94 \pm 0.19	0.22 \pm 0.06	0.09 \pm 0.001	0.03 \pm 0.01
	liver	1.16 \pm 0.09	1.06 \pm 0.35	1.04 \pm 0.18	0.72 \pm 0.16
	kidney	10.84 \pm 1.25	9.07 \pm 0.66	4.19 \pm 0.57	1.63 \pm 0.51
	GI	0.16 \pm 0.03	1.16 \pm 0.4	1.93 \pm 0.37	2.27 \pm 0.59
8	blood	1.03 \pm 0.14	0.45 \pm 0.1	0.22 \pm 0.02	0.09 \pm 0.01
	liver	0.95 \pm 0.14	3.02 \pm 0.59	0.98 \pm 0.22	0.44 \pm 0.14
	kidney	10.79 \pm 1.97	17.05 \pm 3.17	9.52 \pm 2.54	3.94 \pm 0.43
	GI	0.16 \pm 0.01	1.96 \pm 0.49	1.64 \pm 0.64	2.53 \pm 0.70
9	blood	1.00 \pm 0.14	0.35 \pm 0.05	0.19 \pm 0.03	0.14 \pm 0.02
	liver	0.68 \pm 0.06	0.5 \pm 0.14	0.26 \pm 0.04	0.18 \pm 0.03
	kidney	12.8 \pm 1.31	5.68 \pm 1.99	2.38 \pm 0.45	1.09 \pm 0.17
	GI	0.12 \pm 0.02	0.36 \pm 0.11	0.72 \pm 0.11	0.69 \pm 0.19

^a Data are %ID/g, expressed as mean \pm SD.

(>2 %ID/g at 2 h) over the 2 h study period. Interestingly, these neutral complexes are similar in nature to ^{99m}Tc -PAMAK, with one heterocyclic chelating moiety and one acetic acid chelating moiety, and displayed a similar clearance pattern to ^{99m}Tc -PAMAK as well.

^{99m}Tc -SAAC complex **9**, the diacetic acid derivative, exhibited high initial kidney uptake with rapid renal clearance (5.68 \pm 1.99 and 1.09 \pm 0.17 %ID/g at 0.5 and 2 h, respectively) and the least liver and GI accumulation of any of the chelators tested after the initial time point (0.18 \pm 0.03 and 0.69 \pm 0.19 %ID/g at 2 h, respectively). This complex exhibited an ideal pharmacokinetic clearance profile for development into radiopharmaceuticals; however, this chelator was not studied further because of lower RCY.

Table 2. Comparisons of the Partition Coefficients (log *P*) for the ^{99m}Tc-SAAC Complexes

compd	log <i>P</i>
DpK	-1.89
PAMA-K	-1.80
1	-2.00
2	-1.72
3	-1.10
4	-2.33
5	-1.61
6	-0.91
7	-1.75
8	-1.84
9	-2.20
NTA control ^a	-2.88

^a Lipowska et al. (20).

It is clear that despite the rapid clearance from the blood of the first generation of SAAC complexes, ^{99m}Tc-DpK and ^{99m}Tc-PAMAK, a significant portion of their excretion was via the hepatobiliary route, hindering the potential application of these chelators in the development of radiopharmaceuticals. These limitations are realized in the development of cancer imaging agents where the ability to visualize metastatic lesions in the abdominal cavity with a DpK containing chelator is confounded by the high background signal present in the liver and GI. Through the preparation of a variety of novel polar and/or hydrophilic SAAC systems that are inherently less lipophilic, the pharmacokinetic profiles have been successfully altered to favor renal clearance.

Determination of Partition Coefficients (log *P*) as a Measure of Lipophilicity. The log *P* values (Table 2) of the complexes were determined using the HPLC purified ^{99m}Tc-SAAC complexes by the shake flask method utilizing *n*-octanol and 25 mM phosphate buffer (pH 7.4) as the solvents. NTA was tested as a control based on the published results that the ^{99m}Tc-NTA complex undergoes rapid and efficient renal clearance (20).

The lipophilicity of the complexes as measured by the octanol/phosphate buffer (pH 7.4) extinction coefficients followed the general trend of the rat tissue distribution pharmacokinetic profiles whereby the complexes with more negative log *P* values displayed a more desirable pharmacokinetic profile (high kidney/low hepatobiliary clearance). For example, **4** with log *P* of -2.33 cleared primarily by renal excretion, while **7** with a less negative log *P* of -1.75 cleared by combined renal and hepatobiliary routes. However, the correlation between the log *P* measurements and renal uptake and clearance of the radioactive complexes was not perfect because complexes like **3** with a log *P* of -1.10 still have high kidney uptake. Therefore, the log *P* values should only be considered as one of many physiochemical properties of the complexes that govern the in vivo distribution, uptake, metabolism, and excretion.

Incorporation of ^{99m}Tc-SAAC Complexes into Tyr-3-octreotide. One of the most important applications for the SAAC technology is the incorporation of the SAAC ligands directly into clinically relevant peptides. This is readily accomplished using standard solid phase peptide synthesis strategies (8, 29). To that end, we have incorporated two SAAC ligands, DpK and **4**, at the N-terminus of Tyr-3-octreotide, a somatostatin receptor 2 (SSTR2) selective peptide agonist. Following complexation with ^{99m}Tc, we evaluated the tissue distribution for comparison to ¹¹¹In-DOTA-Tyr-3-octreotide, a well established peptide based radiopharmaceutical for the detection of carcinoid and neuroendocrine tumors (30–33). The SAAC ligand, **4**, was selected for evaluation based on the favorable pharmacokinetic profile in rats demonstrating kidney uptake and GI/liver clearance of the ^{99m}Tc-SAAC complex, high RCY, and prolonged

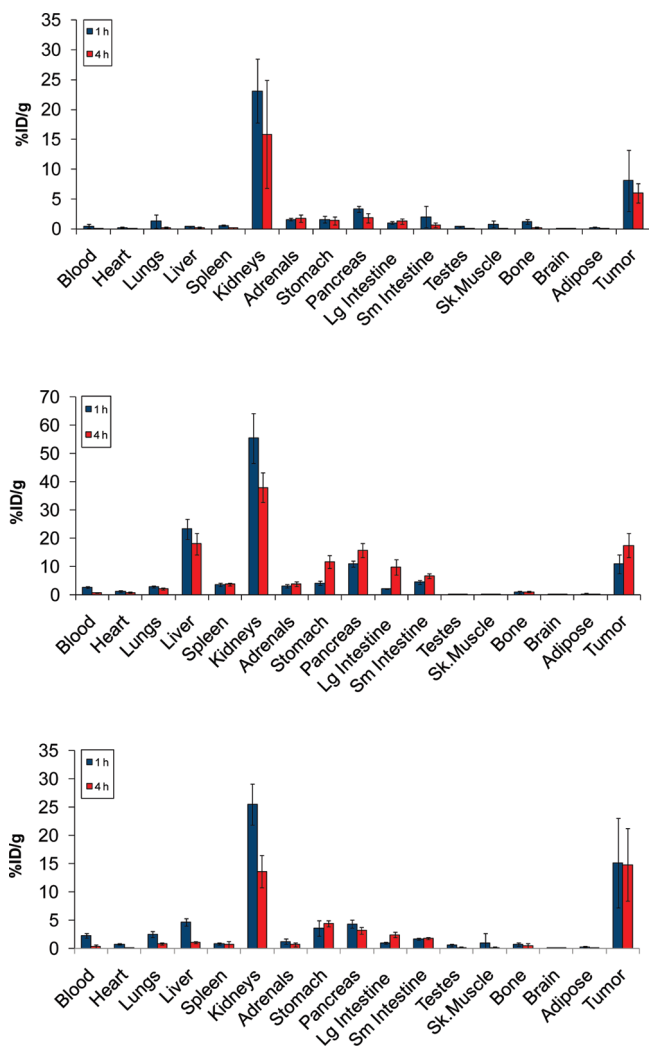


Figure 4. Tissue distribution of SSTR2 receptor mediated ¹¹¹In-DOTA-Tyr-3-octreotide (top) versus ^{99m}Tc-DpK-Tyr-3-octreotide (middle) and ^{99m}Tc-**4**-Tyr-3-octreotide (bottom) in AR42J mouse tumor model.

chemical stability. The incorporation of DpK was used for a direct comparison of a first generation SAAC with similar size. The results of the tissue distributions are shown in Figure 4. While both ^{99m}Tc-DpK-Tyr-3-octreotide and ¹¹¹In-DOTA-Tyr-3-octreotide demonstrate specific uptake and retention in target tissues, tumor and pancreas, the liver and GI uptake of ^{99m}Tc-DpK-Tyr-3-octreotide is significantly greater than that of ¹¹¹In-DOTA-Tyr-3-octreotide, thus highlighting the necessity of developing advanced SAAC ligands with a pharmacokinetic profile that favors renal clearance. In contrast, ^{99m}Tc-**4**-Tyr-3-octreotide exhibited a very similar tissue distribution to the ¹¹¹In-DOTA-Tyr-3-octreotide with high renal clearance and significantly reduced liver uptake of 4.63 ± 0.65 %ID/g at 1 h compared to 23.31 ± 3.5 %ID/g at 1 h for ^{99m}Tc-DpK-Tyr-3-octreotide ($p < 0.001$). Likewise, both the large and small intestines of the ^{99m}Tc-**4**-Tyr-3-octreotide showed reduced radioactivity at both time points examined compared to ^{99m}Tc-DpK-Tyr-3-octreotide. ^{99m}Tc-**4**-Tyr-3-octreotide also exhibited slightly higher tumor uptake at 1 h (15.15 ± 7.92 %ID/g) compared to the ¹¹¹In-DOTA-Tyr-3-octreotide (8.08 ± 5.17 %ID/g) and significantly higher tumor uptake at 4 h compared to ¹¹¹In-DOTA-Tyr-3-octreotide (14.85 ± 6.41 and 5.99 ± 1.65 %ID/g, respectively) ($p < 0.03$). The tumor-to-blood ratio of ^{99m}Tc-**4**-Tyr-3-octreotide was an encouraging 6.7:1 at 1 h and reached a maximum at 4 h with an impressive 35:1 ratio. Thus, the utility of this class of chelators is accentuated by the ability

to maintain high tumor uptake while driving preferential renal clearance of molecules, which would otherwise be dominated by hepatobiliary localization and excretion.

In summary, our ongoing research into the development of novel ^{99m}Tc chelators has led to significant improvements of a key characteristic of the already robust proprietary SAAC radiolabeling platform. The pharmacokinetic profile of the ^{99m}Tc-SAAC metal complex has been significantly altered through the design and synthesis of SAAC systems with the potential to enhance renal clearance and diminish hepatobiliary accumulation and/or clearance. The benefit of the second generation ^{99m}Tc-SAAC technology was realized upon incorporation of ^{99m}Tc-SAAC (4) into Tyr-3-octreotide, resulting in a significant decrease of the ^{99m}Tc-SAAC complex in nontarget and hepatobiliary tissues, thus affording the potential to design and develop a superior ^{99m}Tc-SAAC-Tyr-3-octreotide radioimaging agent with the potential to image cancer with improved whole body clearance. Future efforts will focus on applying the novel polar SAAC chelates to additional biologically relevant peptides and small molecules for the development of novel radiopharmaceuticals to image and potentially treat a variety of diseases.

ACKNOWLEDGMENT

This work was supported in part by grants (J.W.B.) from the Department of Energy (Grant D2-FG02-99ER62791) and the National Institutes of Health (Grant 1R41A1054080-01).

Supporting Information Available: Radiolabeling summary for ^{99m}Tc-1-9 SAAC complexes as well as ^{99m}Tc-4-Tyr-3-octreotide, ^{99m}Tc-DpK-Tyr-3-octreotide, and ¹¹¹In-DOTA-Tyr-3-octreotide including representative radiochromatograms. This material is available free of charge via the Internet at <http://pubs.acs.org>.

LITERATURE CITED

- Mariani, G., Nicolini, M., Wagner, H. W., Eds. (1983) *Technetium in Chemistry and Nuclear Medicine* Vol. 1, Cortina International, Verona, Italy.
- Bartholomae, M., Valliant, J., Maresca, K. P., Babich, J. W., and Zubieta, J. (2009) Single amino acid chelates: a strategy for the design of technetium and rhenium radiopharmaceuticals. *Chem. Commun.* 5, 493–512.
- Jurisson, S. S., and Lyden, J. D. (1999) Potential technetium small molecule radiopharmaceuticals. *Chem. Rev.* 99, 2205.
- Heeg, M. J., and Jurisson, S. (1999) The role of inorganic chemistry in the development of radiometal agents for cancer therapy. *Acc. Chem. Res.* 32 (12), 1053–1060.
- Nicolini, M., Bandoli, G., Mazzi, U., Eds. (2006) *Technetium, Rhenium and Other Metals in Chemistry and Nuclear Medicine* Vol. 7, S. G. Editoriali, Padova, Italy.
- Maresca, K. P., Hillier, S. M., Femia, F. J., Zimmerman, C. N., Levadala, M. K., Banerjee, S. R., Hicks, J., Sundararajan, C., Valliant, J., Zubieta, J., Eckelman, W. C., Joyal, J. L., and Babich, J. W. (2009) Comprehensive radiolabeling, stability, and tissue distribution studies of technetium-99m single amino acid chelates (SAAC). *Bioconjugate Chem.* 20 (8), 1625–1633.
- James, S., Maresca, K. P., Allis, D. G., Valliant, J. F., Eckelman, W., Babich, J. W., and Zubieta, J. (2006) Extension of the single amino acid chelate concept (SAAC) to bifunctional biotin analogues for complexation of the M(CO)₃⁺ core (M = Tc and Re): syntheses, characterization, biotinidase stability, and avidin binding. *Bioconjugate Chem.* 17 (3), 579–589.
- Stephenson, K. A., Zubieta, J., Banerjee, S. R., Levadala, M. K., Taggart, L., Ryan, L., McFarlane, N., Boreham, D. R., Maresca, K. P., Babich, J. W., and Valliant, J. F. (2004) A new strategy for the preparation of peptide-targeted radiopharmaceuticals based on an Fmoc-lysine-derived single amino acid chelate (SAAC). Automated solid-phase synthesis, NMR characterization, and in vitro screening of fMLF(SAAC)G and fMLF[(SAAC-Re-(CO)₃)⁺]G. *Bioconjugate Chem.* 15 (1), 128–136.
- Stephenson, K. A., Banerjee, S. R., Besanger, T., Sogbein, O. O., Levadala, M. K., McFarlane, N., Lemon, J. A., Boreham, D. R., Maresca, K. P., Brennan, J. D., Babich, J. W., Zubieta, J., and Valliant, J. F. (2004) Bridging the gap between in vitro and in vivo imaging: isostructural Re and ^{99m}Tc complexes for correlating fluorescence and radioimaging studies. *J. Am. Chem. Soc.* 126 (28), 8598–8599.
- D'Andrea, L. D., Testa, I., Panico, M., Di Stasi, R., Caraco, C., Tarallo, L., Arra, C., Barbieri, A., Romanelli, A., and Aloj, L. (2008) In vivo and in vitro characterization of CCK8 bearing a histidine-based chelator labeled with ^{99m}Tc-tricarbonyl. *Biopolymers* 90 (5), 707–712.
- Alberto, R., Schibli, R., Waibel, R., Abram, U., and Schubiger, A. P. (1999) Basic aqueous chemistry of [M(OH)₂(CO)₃]⁺ (M=Re, Tc) directed towards radiopharmaceutical application. *Coord. Chem. Rev.* 190–192, 901–919.
- Schibil, R., La Bella, R., Alberto, R., Garcia-Garayoa, E., Ortner, K., Abram, U., and Schubiger, P. A. (2000) Influence of the denticity of ligand systems on the in vitro and in vivo behavior of ^{99m}Tc(I)-tricarbonyl complexes: a hint for the future functionalization of biomolecules. *Bioconjugate Chem.* 11, 345–351.
- Pietzsch, H.-J., Gupta, A., Reisgys, M., Drews, A., Seifert, S., Syhre, R., Spies, H., Alberto, R., Abram, U., and Schubiger, P. A. (2000) Chemical and biological characterization of technetium(I) and rhenium(I) tricarbonyl complexes with dithioether ligands serving as linkers for coupling the Tc(CO)₃ and Re(CO)₃ moieties to biologically active molecules. *Bioconjugate Chem.* 11 (3), 414–424.
- Bourkoula, A., Paravatou-Petsotas, M., Papadopoulos, A., Santos, I., Pietzsch, H.-J., Livanou, E., Pelecanou, M., Papadopoulos, M., and Pirmettis, I. (2009) Synthesis and characterization of rhenium and technetium-99m tricarbonyl complexes bearing the 4-[3-bromophenyl]quinazoline moiety as a biomarker for EGFR-TK imaging. *Eur. J. Med. Chem.* 44 (10), 4021–4027.
- Maria, L., Fernandes, C., Garcia, R., Gano, L., Paulo, A., Santos, I. C., and Santos, I. (2009) Tris(pyrazolyl)methane ^{99m}Tc tricarbonyl complexes for myocardial imaging. *Dalton Trans.* (4), 603–606.
- Lu, G., Hillier, S. M., Maresca, K. P., Zimmerman, C. N., Wang, J., Shay, C., Marquis, J. C., Eckelman, W. C., Joyal, J. L., and Babich, J. W. (2009) Small molecule carbonic anhydrase IX inhibitors with Re/Tc for targeted molecular imaging of cancer. *Abstracts of Papers*, 238th National Meeting of the American Chemical Society, Washington, DC, August 16–20, American Chemical Society, Washington, DC.
- Femia, F. J., Maresca, K. P., Hillier, S. M., Zimmerman, C. N., Joyal, J. L., Barrett, J. A., Aras, O., Dilsizian, V., Eckelman, W. C., and Babich, J. W. (2008) Synthesis and evaluation of a series of ^{99m}Tc(CO)₃⁺ lisinopril complexes for in vivo imaging of angiotensin-converting enzyme expression. *J. Nucl. Med.* 49 (6), 970–977.
- Lipowska, M., He, H., Malveaux, E., Xu, X., Marzilli, L. G., and Taylor, A. (2006) First evaluation of a ^{99m}Tc-tricarbonyl complex, ^{99m}Tc(CO)₃(LAN), as a new renal radiopharmaceutical in humans. *J. Nucl. Med.* 47 (6), 1032–1040.
- He, H., Lipowska, M., Christoforou, A., Marzilli, L. G., and Taylor, A. T. (2007) Initial evaluation of new ^{99m}Tc(CO)₃ renal imaging agents having carboxyl-rich thioether ligands and chemical characterization of Re(CO)₃ analogues. *Nucl. Med. Biol.* 34 (6), 709–716.
- Lipowska, M., Marzilli, L. G., and Taylor, A. T. (2009) ^{99m}Tc(CO)₃-nitritoltriacetic acid: a new renal radiopharmaceutical showing pharmacokinetic properties in rats comparable to those of ¹³¹I-OIH. *J. Nucl. Med.* 50, 454–460.
- Maresca, K. P., Kronauge, J. F., Zubieta, J., and Babich, J. W. (2007) Novel ether-containing ligands as potential ^{99m}technetium(I) heart agents. *Inorg. Chem. Commun.* 10 (12), 1409–1412.

- (22) Maresca, K. P., Keith, D., Femia, F. J., Graham-Coco, W. A., Kronauge, J. F., Sogbein, O. O., Valliant, J., Babich, J. W. (2006) SAR development of ether-containing ligand complexes of $\text{Tc}(\text{CO})_3^+$ for cardiac imaging. In *Technetium in Chemistry and Nuclear Medicine*, 7th ed. (Mazzi, U., Ed.) pp 399–402, S. G. Editoriali, Padova, Italy.
- (23) Shah, T., Kulakiene, I., Quigley, A., Warbey, V. S., Srirajskanthan, R., Toumpanakis, C., Hochhauser, D., Buscombe, J., and Caplin, M. E. (2008) The role of $^{99\text{m}}\text{Tc}$ -depreotide in the management of neuroendocrine tumours. *Nucl. Med. Commun.* 29 (5), 436–440.
- (24) Quigley, A., Buscombe, J. R., Shah, T., Gnanasegaran, G., Roberts, D., Caplin, M. E., and Hilson, A. J. W. (2005) Intertumoural variability in functional imaging within patients suffering from neuroendocrine tumours. *Neuroendocrinology* 82 (3–4), 215–220.
- (25) Kowalski, J., Henze, M., Schuhmacher, J., Macke, H. R., Hofmann, M., and Haberkorn, U. (2003) Evaluation of positron emission tomography imaging using [^{68}Ga]-DOTA-D Phe(1)-Tyr(3)-octreotide in comparison to [^{111}In]-DTPAOC SPECT. First results in patients with neuroendocrine tumors. *Molecular Imaging Biol.* 5 (1), 42–48.
- (26) Yao, Z., Bhaumik, J., Dhanalekshmi, S., Ptaszek, M., Rodriguez, P. A., and Lindsey, J. S. (2007) Synthesis of porphyrins bearing 1–4 hydroxymethyl groups and other one-carbon oxygenic substituents in distinct patterns. *Tetrahedron* 63, 10657–10670.
- (27) Schweinsberg, C., Maes, V., Brans, L., Blauenstein, P., Tourwe, D. A., Schubiger, P. A., Schibli, R., and Garayoa, E. G. (2008) Novel glycosylated [$^{99\text{m}}\text{Tc}(\text{CO})_3$]-labeled bombesin analogues for improved targeting of gastrin-releasing peptide receptor-positive tumors. *Bioconjugate Chem.* 19 (12), 2432–2439.
- (28) Yang, C.-T., Kim, Y.-S., Wang, J., Wang, L., Shi, J., Li, Z.-B., Chen, X., Fan, M., Li, J.-J., and Liu, S. (2008) ^{64}Cu -labeled 2-(diphenylphosphoryl)ethyl-diphenylphosphonium cations as highly selective tumor imaging agents: effects of linkers and chelates on radiotracer biodistribution characteristics. *Bioconjugate Chem.* 19 (10), 2008–2022.
- (29) Smith, C. J., Gali, H., Sieckman, G. L., Higginbotham, C., Volkert, W. A., and Hoffman, T. J. (2003) Radiochemical investigations of $^{99\text{m}}\text{Tc}$ -N3S-X-BBN[7–14] NH_2 ; an in vitro/in vivo structure–activity relationship study where X = 0, 3, 5, 8, and 11-carbon tethering moieties. *Bioconjugate Chem.* 14, 93–102.
- (30) De Jong, M., Breeman, W. A. P., Kwekkeboom, D. J., Valkema, R., and Krenning, E. P. (2009) Tumor imaging and therapy using radiolabeled somatostatin analogues. *Acc. Chem. Res.* 42 (7), 873–880.
- (31) Oeberg, K. (2008) Molecular imaging of neuroendocrine tumors. *Expert Rev. Endocrinol. Metab.* 3 (6), 739–749.
- (32) Goldsmith, S. J. (2009) Update on nuclear medicine imaging of neuroendocrine tumors. *Future Oncol.* 5 (1), 75–84.
- (33) Reubi, J. C., and Maecke, H. R. (2008) Peptide-based probes for cancer imaging. *J. Nucl. Med.* 49 (11), 1735–1738.

BC900517X